Addition of Benzoyl Radicals to Butyl Acrylate: Absolute Rate Constants by Time-Resolved EPR

Daniela Hristova,[†] Iwo Gatlik,[‡] Günther Rist,[‡] Kurt Dietliker,[§] Jean-Pierre Wolf,[§] Jean-Luc Birbaum,[§] Anton Savitsky,[⊥] Klaus Möbius,[⊥] and Georg Gescheidt*,[†]

Institute of Physical and Theoretical Chemistry, Graz University of Technology, Technikerstrasse 4, A-8010 Graz, Austria; Department of Chemistry, Physical Chemistry, University of Basel, Klingelbergstrasse 80, 4056 Basel, Switzerland; Ciba Specialty Chemicals Inc., 4002 Basel, Switzerland; and Institute of Experimental Physics, Free University of Berlin, Arnimallee 14, 14195 Berlin, Germany

Received August 12, 2004; Revised Manuscript Received June 14, 2005

ABSTRACT: The addition rate constants of five differently substituted benzoyl radicals to butyl acrylate were determined by continuous-wave time-resolved EPR (TR-EPR at X-band (9 GHz) and at W-band (95 GHz)) spectroscopy. Remarkably, the reactivity of the benzoyl radicals, is divided into two domains: One is established at low (<1.25 M) concentrations of butyl acrylate with rate constants in the range of 10^6 mol^{-1} s^{-1}. At alkene concentrations above ca. 1.25 M, the addition reaction slows down by ~1 order of magnitude. This decrease of the reactivity coincides with a dramatic increase of the macroscopic viscosity in the reaction medium.

Introduction

Photoinitiators have been utilized in a variety of technological applications ranging from coatings to dentistry. A very common molecular constituent of such initiators is a (substituted) benzoyl moiety which is responsible for the formation of excited triplet π,π^* states and, as a consequence, triggers an α-cleavage reaction.[1] This is illustrated in Scheme 1 for a monoacyl phosphinoxide and an α-amino ketone. Both types of photoinitiators undergo intersystem crossing (ISC) and cleave in the triplet state. A benzoyl radical (**B**) is formed along with a phosphinoyl (**P**) or an α-amino C-centered radical (**C**), and both radicals are able to initiate polymerization.[2−6] The addition of these primary radicals to an alkene affords the carbon-centered radicals **BC**, **PC** (for phosphinoxides), and **CC** (for α-amino ketones) as the first segments of a polymerization (Scheme 2). This first reaction step is representative for the efficiency of a photoinitiator, and therefore, the kinetics for this reaction are of particular interest. Kinetic data for several phosphinoyl and α-amino C-centered radicals are available.[7−11] Remarkably, information on benzoyl radicals, the most frequently occurring radicals in α-cleavage reactions, is only scarce,[12−14] although their reactivity toward C=C double bonds and, e.g., oxygen is of crucial importance. This lack of information exists because the optical absorption of benzoyl radicals is hardly detectable by UV−vis spectroscopy, and only few studies made use of time-resolved IR.[12,13,15] However, benzoyl radicals can readily be detected by continuous-wave (CW) EPR spectroscopy. Nevertheless, this latter technique was only in rare cases utilized for kinetic studies since the EPR signal intensities obtained in the time-resolved (nanosecond) regime are, in general, not proportional to the radical concentrations but are also affected by spin-polarization effects which cause that the magnetic levels responsible for the EPR transitions are not populated in a Boltzmann equilibrium.[16]

Scheme 1. Formation of the Primary Radicals from Acylphosphinoxide and α-Aminoketone-Type Photoinitiators (ISC = Intersystem Crossing)

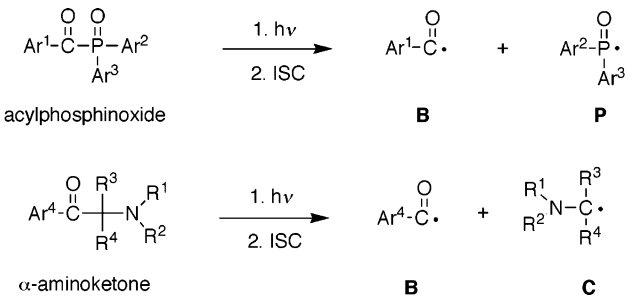

Recently, we have shown that absolute rate constants of photoinitiator radicals can readily be determined by line-width measurements in continuous-wave time-resolved EPR spectra at X-band (CW TR-EPR, 9 GHz).[11] This approach is based on the fact that radical decay occurring by first-order chemical reaction contributes linearly to the effective transversal relaxation rate $1/T_2^*$. The method is related to previous kinetic studies by pulsed time-resolved EPR.[17−19]

Assuming a chemical reaction to obey a pseudo-first-order rate law, it can be shown that

$$1/T_2^* = 1/T_2^0 + k_{add}[M] \quad (1)$$

where T_2^0 represents the transversal relaxation time without added quencher, T_2^* is the transversal relaxation time (both values are determined by simulations of the EPR lines), k_{add} is the first-order rate constant of the quenching reaction, and [M] is the concentration of the quencher (here butyl acrylate). It has been recently shown that eq 1 holds for CW- and FT-EPR (X-band).[7]

This method has been successfully used for the determination of absolute quenching rate constants of

† Graz University of Technology.
‡ University of Basel.
§ Ciba Speciality Chemicals, Inc.
⊥ Free University of Berlin.
* Corresponding author: Fax +43 316 8738225; e-mail gescheidt@ptc.tugraz.at.

10.1021/ma0483367 CCC: $30.25
Published on Web 08/04/2005

Scheme 2. Origin of Radicals PC, BC, and CC

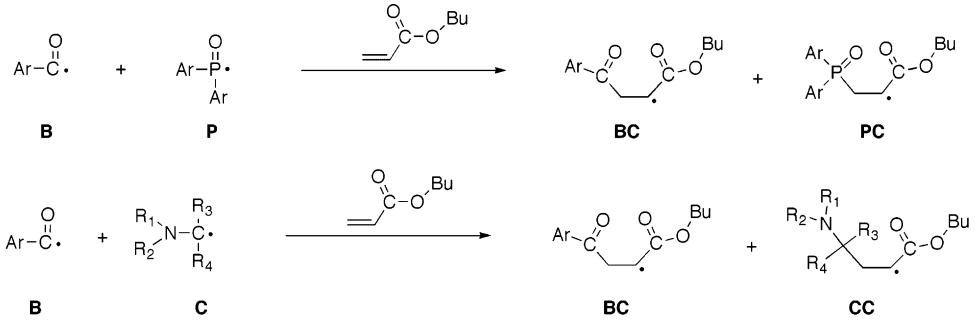

Chart 1. Photoinitiators 1−5 and the Radicals Formed upon the Cleavage of the α-Carbonyl Bond[a]

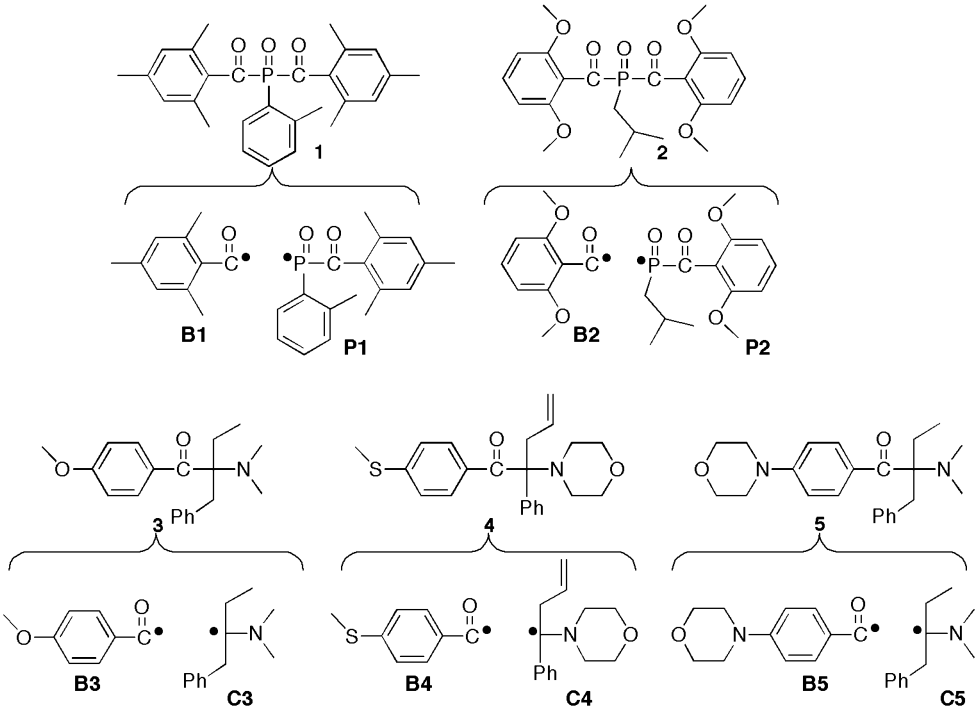

[a] Benzoyl radicals are denoted B1−B5, phosphorus-centered P1 and P2, and carbon-centered C3−C5, according to the parent photoinitiators.

phosphinoyl radicals.[11] However, it still remains a challenge to establish the reactivity of benzoyl radicals. Although their EPR signals are readily detectable, their kinetic analysis is not easy. This is because the benzoyl radicals, in general, react much slower than, e.g., the phosphinoyl radicals.[20] Accordingly, the line-width variations ($1/T_2^* - 1/T_2^0$) depending on the quencher concentration in the CW-TR-EPR spectra become smaller, causing bigger error margins. This can be overcome by increasing the number of measurements and data points for the analysis.

Alternatively, time-resolved EPR at high field (W-band, 95 GHz) allows the evaluation of the chemical lifetime of the observed species directly from the time profiles of the EPR intensities. At high magnetic field (3.4T), the population difference of the spin energy levels is increased by the factor of 10 compared with X-band (0.34 T). Taking into account that spin polarization in our systems remains constant or even (more likely) decreases at high field, the kinetic constants representing the chemical reaction can be directly established from the EPR signal decays.[21] Consequently, two EPR approaches are envisaged to determine the chemical lifetime from eq 1: to measure the line broadening $1/T_2^* - 1/T_2^0$ by X-band EPR when varying [M] or to measure the time profile of W-band EPR intensities depending on [M].

Hence, in a first step, we have investigated the addition of benzoyl radicals to butyl acrylate in more detail by continuous-wave TR-EPR at X-band. To verify these results particularly at low butyl acrylate concentrations, in a second step, reference measurements at W-band were performed.

There is, however, an additional complication which occurs when the second constituent of the primarily formed radical pair has a considerably higher reactivity than the benzoyl radical, e.g., an unsubstituted phosphinoyl radical: The alkene is predominately consumed by the phosphinoyl radical; this may result in the addition of the benzoyl radical to the acrylate not always following a simple first-order rate law.

Such difficulties were avoided by selecting initiators with addition constants of the second primary radical as small as possible. Photoinitiators **1**−**5** (Chart 1) are ideally suited for these studies. The photolysis of **1**−**5** yields five different benzoyl radicals with an 2,4,6-trimethylphenyl (**B1**), 2,6-dimethoxyphenyl (**B2**), 4-methoxyphenyl (**B3**), 4-thiomethylphenyl (**B4**), and 4-morpholinophenyl (**B5**) substituent (see Scheme 1). It was shown in previous investigations that the phosphinoyl

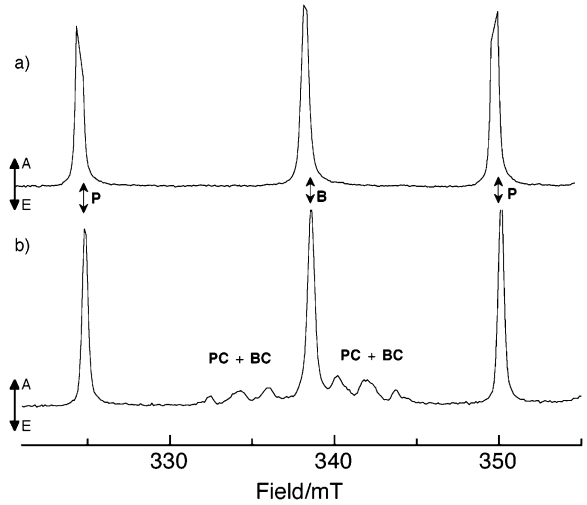

Figure 1. X-band TR-EPR spectra of **1** (0.01 M) in toluene (a) without and (b) with butyl acrylate (2.8 M) observed 200−300 ns after the laser flash.

radicals **P1** and **P2** possess relatively low addition constants of 8×10^5 and 1.8×10^6 M^{-1} s^{-1} to butyl acrylate, respectively, due to the steric hindrance of the radical center by the substituents in the aryl (or, for **P1**, branched alkyl) groups.[11] The same is true for the α-amino C-centered radicals **C3** (identical to **C5**) and **C4** (6.1×10^6 and 1×10^5 M^{-1} s^{-1}, respectively).

Experimental Section

The photoinitiators **1**−**5** were obtained from Ciba Specialty Chemicals Inc. Toluene and butyl acrylate were obtained from Fluka in their purest available form and used without further purification. All experiments were carried out at room temperature.

X-Band EPR. The compounds were dissolved in toluene (0.005−0.01 M, optical density ca. 0.5), and the solutions were saturated with argon or helium. Butyl acrylate (Fluka purum) was used in concentrations between 0.3 and 2.8 M. A home-built flow system was used consisting of a cylindrical quartz cell (diameter 4 mm) and Teflon tubing to connect the pump system (Reglo digital pump, Ismatec, Glattbrugg, Switzerland). It provides a fast, turbulent flow. TR-EPR experiments were performed without modulation of the external magnetic field on a Bruker ESP 300E spectrometer equipped with a microwave amplifier, a TE_{102} microwave cavity (microwave power 9 mW, response time 40 ns). The response of the EPR spectrometer after a laser pulse at a fixed value of the static magnetic field was stored in a LeCroy 9400 dual 125 MHz digital oscilloscope. The central control unit consists of a PC computer with a Debian Linux operating system and a GPIB interface board. The experiment is controlled by the program fsc2 (J. T. Toerring, Institut fuer Experimentalphysik, Freie Universitaet Berlin). A Continuum Surelite II, Nd:YAG laser with a fixed repetition frequency of 20 Hz (4−6 ns pulse width, frequency-tripled, 355 nm) was used as the light source. For each photoinitiator and each concentration of the butyl acrylate, the experiment was performed four times (freshly prepared reaction solutions). Within the period of constant EPR line width, the signal attributed to the benzoyl radical was simulated for 10 slices along the magnetic field. Thus, a set of 40 values led to the average line width represented in Figure 4 (The error bars show individual errors for each data point, determined from the standard deviation of the fit procedure.) The error margins of the addition constants given in Table 1 contain the contributions of the line fit and linear-regression errors. The simulations of the EPR signals were performed with a home-built routine using Matlab (Version 6, Mathworks Inc., Natick). T_2^{*-1} values were directly determined from the least-squares fit of the Gauss-type EPR signals.

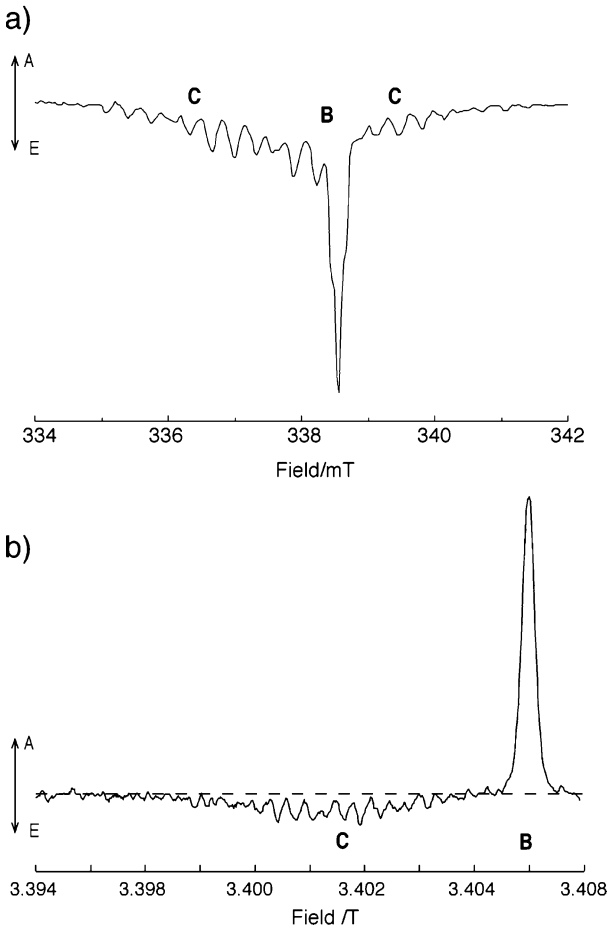

Figure 2. TR-EPR spectra recorded after laser flash photolysis of **5** in toluene in the absence of butyl acrylate: (a) X-band spectrum: 9 mM of **5**, 900 ns time delay; (b) W-band spectrum: 9 mM of **5**, 200 ns time delay (A = absorption, E = emission). For details, see text.

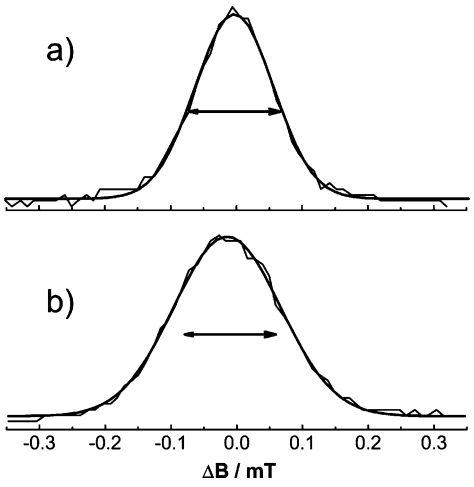

Figure 3. X-band TR-EPR spectra of the benzoyl radical **B5** recorded 600 ns after the laser flash (thin lines): (a) butyl acrylate concentration 0 M; (b) butyl acrylate concentration 2.8 M. The solid lines show their simulation by a Gauss function with the half-width, $\Delta B_{1/2} = 0.0842$ (a) and 0.0947 mT (b). The arrows in (a) and (b) possess identical lengths and indicate the amount of the line broadening.

W-Band EPR. The photoinitiators were dissolved in toluene (0.01−0.05 M; optical density 0.6). The solutions were deoxygenated by purging with argon for 30 min prior to the measurements. The W-band time-resolved experiments were performed with a laboratory-built high-field EPR spectrometer

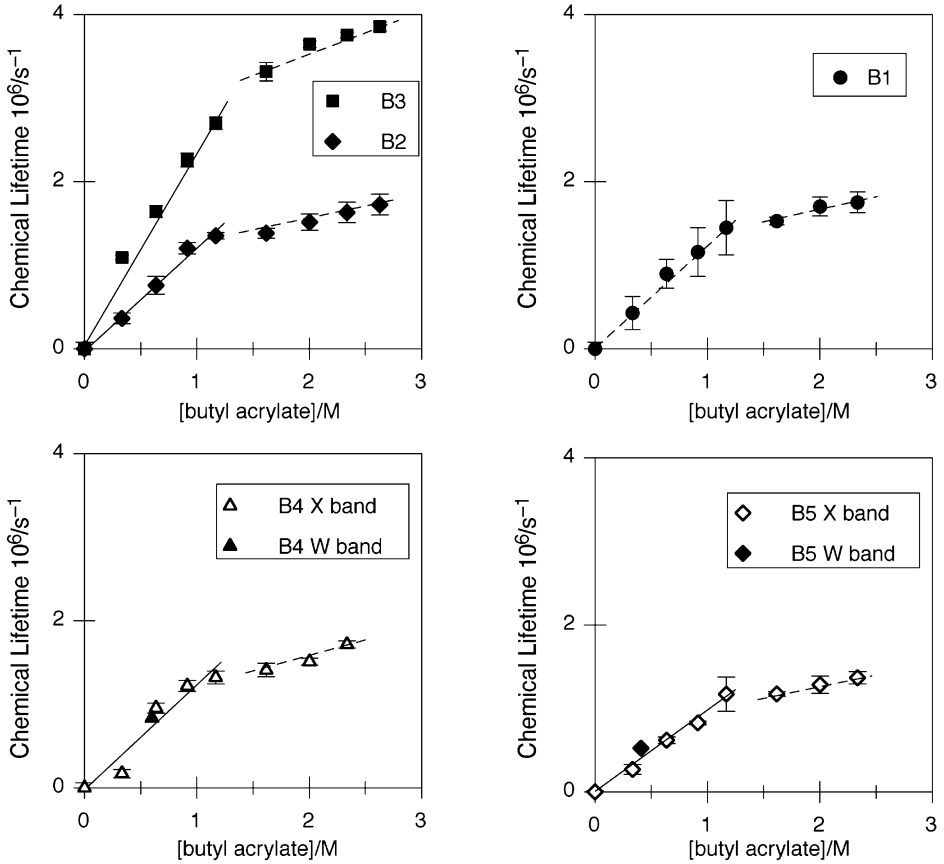

Figure 4. Plots of the chemical lifetimes vs concentration for the determination of k_{add} from TR-EPR spectra at X and W band for benzoyl radicals **B1**−**B5**. The linear relationships for butyl acrylate concentrations < 1.25 M are indicated as solid lines, and those for higher concentrations with dashed lines.

Table 1. *g* Factors and Addition Rate Constants, k_{add}, of Benzoyl Radicals B1−B5 to Butyl Acrylate, Determined by TR-EPR at 9 and 95 GHz (Solvent, Toluene; Room Temperature)[a]

benzoyl radical	*g*-factor	$k_{add}/10^6$ mol^{-1} s^{-1} 0.0−1.25 M butyl acrylate concn	$k_{add}/10^5$ mol^{-1} s^{-1} 1.26−2.7 M butyl acrylate concn
B1	2.000 55	1.18 ± 0.07	4.3 ± 0.7
B2	2.000 57	1.25 ± 0.05	4.6 ± 0.7
B3	2.000 90	1.91 ± 0.01	7.1 ± 0.2
B4	2.000 77	1.25 ± 0.05	5.7 ± 0.8
B5	2.000 86	1.03 ± 0.07	3.6 ± 0.5

[a] The absolute error in *g*-factor measurements is $\pm 5 \times 10^{-5}$.

of 10 ns response time, operating at about 95 GHz and using a cylindrical TE_{011} optical transmission cavity.[22] A superconducting magnet (Cryomagnetics) provides a maximum field of 6 T. The sample quartz capillary, i.d. = 0.6 mm, o.d. = 0.85 mm, was positioned along the axis of the cavity. The output of a Nd:YAG laser (Spectra Physics) operating at 355 nm was coupled into the cavity by means of a quartz fiber of 0.8 mm diameter. The laser pulse repetition frequency was generally set to 10 Hz, and the output energy was attenuated to a maximum of 1 mJ at the sample surface. The sample solutions were pumped through the capillary by a motor-driven syringe with a flow rate of 0.6 μL/s in order to supply fresh sample material to the light-irradiated cavity volume after every six laser shots. Butyl acrylate was used in concentrations between 0 and 0.6 M. For solutions containing more than 0.6 M butyl acrylate, the high dielectric losses of the sample cause problems with the microwave coupling of the cavity, thus impairing W-band measurements. All experiments were carried out at microwave field strengths up to $\omega_1 = 10^6$ rad s^{-1} to exclude any ω_1 effects on the time profiles.The *g*-values of the transient radicals were determined as previously described.[21]

Viscosity Measurements. The macroscopic kinematic viscosity was measured with a Ubbelohde capillary viscosimeter. After completion of the TR-EPR measurements (irradiation of the solutions for 10 min at 355 nm), the reaction solution (20 mL; initiator, butyl acrylate, toluene) was filled into the appropriate viscosimeter, and the flow time through the capillary was measured. The kinematic viscosity was determined by multiplying the time with the capillary constant.

Quantum mechanical calculations were performed with the Gaussian98 package.[23] All structures were fully optimized with UB3LYP/6-31G*. The minimum-energy paths for the addition reactions were traced by choosing the distance *r* between the β-carbon atom of the *n*-butyl acrylate and the carbon-centered radical as the principal reaction coordinate. The transition states for the addition of the radicals were optimized to evaluate the activation barrier height. Subsequently, single-point calculations were performed at the obtained geometries, using different methods and a variety of basis sets (see Supporting Information). At a fixed level of theory (B3LYP, HF, MP2), the activation barrier was calculated as the electronic energies difference between the saddle point and the minimum structures. Basis set superposition errors were calculated using the counterpoise procedure.

Results and Discussion

X-Band EPR. Shape of the TR-EPR Spectra. Laser flash photolysis of **1**−**5** yields EPR spectra that consist of two components. For the radical pairs generated from **1** and **2**, the EPR signals of the phosphinoyl and the benzoyl radical species are well separated due to the dominating isotropic hyperfine coupling constant (hfc) of the ^{31}P nucleus: The two lines at the edges of the spectra stem from the phosphinoyl radical (**P**) whereas the central line represents the benzoyl radical

(**B**) (Scheme 1, Figure 1a). In the short time regime after excitation of the photoinitiator and α-cleavage, the overall spin in the radical pair has to be identical to its precursor. In this spin-correlated radical pair, the magnetic levels are not populated at thermal equilibrium. Therefore, the EPR signal intensities are not proportional to radical concentrations (particularly not in X-band EPR spectra, see below). Two mechanisms, the radical pair and the triplet polarization, contribution determine the intensities of the EPR lines. Whereas the radical-pair mechanism causes an absorption/emission (or vice versa) pattern of multiplets in EPR spectra, the triplet mechanism leads to enhanced absorption (or emission) of all lines. Depending on the time interval in which a chemical reaction is observed, both mechanisms can become active.

When butyl acrylate is added to the solution containing the photoinitiators **1**−**5**, two more products emerge in the TR-EPR signal (see, e.g., Figure 1b). They represent the C-centered radicals **PC** (for **1** and **2**) or **CC** (for **3**−**5**) and **BC**, in which the phosphinoyl (**P**) or C-centered (**C**) and the benzoyl (**B**) radical have added to one butyl acrylate monomer (Scheme 2).

The X-band EPR signals of the **C**, **PC**, **CC**, and **BC** radicals partially overlap with those of the benzoyl radicals **B**. Nevertheless, the sharp signal of the benzoyl radical is distinguishable, and its line width is not substantially affected by the overlap of EPR lines (Figures 1b and 2a). These observations are crucial for the kinetic investigation of benzoyl radicals by means of the TR-EPR line-width method (eq 1).

X-band EPR. Kinetic Analysis for the Benzoyl Radicals. At X-band, the line broadening of the well-distinguishable TR-EPR resonances of the benzoyl radicals (**B**) can be readily followed when changing the quencher concentration. In Figure 3, the TR-EPR signals of the benzoyl radicals, obtained after photolysis of **1** at two different concentrations of butyl acrylate, are shown together with their simulations.

Line-width analysis of the TR-EPR spectra according to eq 1 yields the plots of chemical lifetime vs concentration displayed in Figure 4. Clearly, a simple linear relationship between the butyl acrylate concentration and the EPR line width for the benzoyl radical is *not* pertinent for the whole range of quencher concentrations. Whereas a linear regression for butyl acrylate concentrations below 1.25 M provides, from the slopes, addition constants, k_{add}, of around 10^6 mol^{-1} s^{-1} (Table 1), at concentrations higher than 1.25 M, the curves level off, and the k_{add} values decrease drastically by up to an order of magnitude.

Addition constants in the range of 10^5−10^6 mol^{-1} s^{-1} are at the limit to be measured by the EPR line-width method because the additional broadening of the EPR lines becomes too small to be detectable by X-band TR-EPR. Moreover, the partial overlap with the spectra of the partner radicals **C** and the products **CC** (Schemes 1 and 2) leads to errors in the line-shape analysis. To obtain reference data and to verify the kinetic constants acquired from the X-band TR-EPR spectra, we have additionally performed TR-EPR experiments at high microwave frequency (W-band).

W-Band EPR. Shape of the TR-EPR Spectra. In the W-band EPR spectra, the signals belonging to different radicals with different *g*-factors show a better separation than at X-band due to the increased Zeeman interaction at 10 times higher magnetic fields. This increased resolution is apparent in Figure 2b where the signal of the 4-morpholinobenzoyl radical **B5** is well separated from that of the 1-phenyl-2-(dimethylamino)-but-2-yl radical **C5**. Moreover, the W-band spectrum, taken 200 ns after the laser pulse, demonstrates strongly increased spin relaxation at high magnetic field owing to field-dependent fluctuating Zeeman and spin-rotation interactions.[24] Because of fast relaxation,[25] the signal of the benzoyl radical **B5** exhibits practically no transient spin polarization whereas that of the carbon-centered radical **C5** is still polarized by the radical pair mechanism.[26,27]

W-Band EPR. Kinetic Analysis for the Benzoyl Radical. As was demonstrated earlier, the line intensities in the W-band spectra of the benzoyl radicals are virtually free from polarization phenomena (vide supra) and represent the observed radicals in thermal equilibrium.[21] Thus, the chemical decay rate of the benzoyl radical can be directly determined by recording the time profile of the EPR signal intensity (cf. Supporting Information). This is accomplished by subtracting the decay curves, evaluated for the pure photoinitiator (with no butyl acrylate present), from those obtained in the presence of butyl acrylate (Figure 4). Because of the high polarity of the reaction solutions at high butyl acrylate concentrations, the W-band experiments could only be run at low concentrations of the alkene when the solutions were not too lossy for the microwaves (see Experimental Part). The chemical lifetimes of the radicals at selected concentrations of butyl acrylate measured by the decay of the high-field line intensities are displayed in Figure 4 together with the results of the X-band measurements. They are in excellent agreement, thus approving the analysis of the X-band EPR spectra, which could be recorded over the complete range of butyl acrylate concentrations.

Reactivity Considerations. Which factors within the dynamic processes are likely to be responsible for the apparent two reactivity/concentration domains of the benzoyl radicals? (i) The rate law of the reaction could change with increasing viscosity caused by a high monomer concentration: In principle, as mentioned in the Introduction, an important portion of the acrylate molecules is consumed by the phosphinoyl or carbon-centered radical, and a second-order rate law could follow for the benzoyl radicals. This, however, is rather unlikely since this effect should be attenuated at high monomer concentrations. Indeed, simulation for the addition reaction of the benzoyl radicals to butyl acrylate for a second-order kinetic scheme showed no reasonable fit to the experimental curve (Figure 4). Moreover, in the case of a second-order reaction, different concentrations of the initiating radicals should influence the line width. Remarkably, variation of the initiating radical concentration, either by photolyzing photoinitiator solutions of differing concentrations or by varying the laser light intensity, did not lead to any changes of the X-band EPR line widths or W-band EPR decay profiles. Thus, a second-order rate law can be ruled out. (ii) The physical properties of the reaction mixture, particularly viscosity, change with acrylate concentration, leading to a reduced reactivity of the benzoyl radicals.[28]

To examine the latter hypothesis, we have measured, over the full concentration range, the viscosity of the solutions used for the TR-EPR measurements (after photolysis). Addition of TEMPO (a stable nitroxide

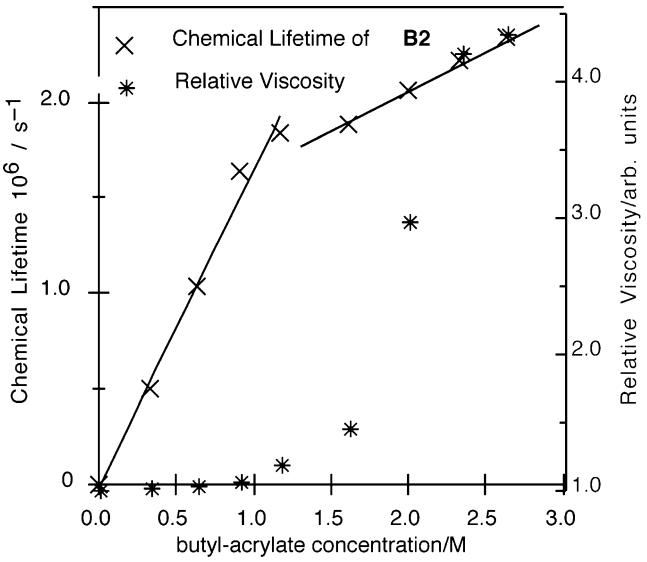

Figure 5. Comparison between the dependencies of the rate constants and the relative kinematic viscosities vs butyl acrylate concentration for **B2**.

radical which can be utilized for the measurement of microscopic mobilities) to the reaction solution did not lead to any anisotropic features of its three-line EPR spectrum, revealing that the local mobility of the radicals is still unaffected (TEMPO is of compatible size as the photoinitiator radicals). Moreover, changes in the spin−spin relaxation times can be neglected within this viscosity range.[25,29] The relative macroscopic kinematic viscosity (determined by capillary viscosimetry) drastically increases at butyl acrylate concentrations > 1.25 M (Figure 5). In parallel, the linear relationship between the chemical lifetime of the benzoyl radical and acrylate concentration is altered: The reactivity of the benzoyl radical toward butyl acrylate is reduced by ~1 order of magnitude at high viscosity.

Therefore, the reactivity of benzoyl radicals can be divided into two domains. At butyl acrylate concentrations below 1.25 M, the first-order rate constants are ca. 1 order of magnitude larger than at quencher concentrations above 1.25 M (Table 1). It is gratifying that the values determined for radicals **B1**, **B2**, **B4**, and **B5** in the high-viscosity range by EPR correspond very well with the values determined by time-resolved IR spectroscopy at high concentrations of butyl acrylate.[14]

Unfortunately, it is not possible to compare the behavior of the benzoyl radicals with that of the phosphinoyl and the α-amino C-centered radicals at high monomer concentrations: The latter are more reactive toward butyl acrylate; therefore, the decay of the corresponding EPR signals is too fast to be observable in the time window of our experiment.

Structure−Reactivity Considerations. The data for the low-viscosity domain (i.e., low acrylate concentration) shown in Table 1 indicate that the rate constant depends on the substituents of the phenyl moiety. It is highest for the 4-methoxybenzoyl radical (**B3**) and lowest for the 4-morpholinobenzoyl (**B5**) derivative. It is tempting to correlate the experimentally established reactivity with molecular properties of the radicals. Indeed, calculations on the UB3LYP/6-31G* level of DFT theory reveal that the s spin population at the carbonyl C atoms is highest for **B3** and lowest for **B5**, correlating with their reactivity. Bearing in mind the relatively small differences between the kinetic constants of **B1**, **B2**, and **B4** and considering additional factors (e.g., steric hindrance) that influence the reactivity of the benzoyl radicals, a dominant correlation between spin distributions and reactivity seems to be too simplistic to rationalize the observed reactivity of these initiators. Therefore, we have calculated the activation barrier heights for the addition of butyl acrylate to the five carbon-centered radicals. Since the unrestricted wave functions of the transition states suffer from severe spin contamination, single-point calculations with ROMP2/6-31G* have been performed for all geometries. The barrier heights are 77.0 (**B1**), 64.7 (**B2**), 46.2 (**B3**), 46.5 (**B4**), and 72.7 kJ/mol (**B5**). These results show a straightforward agreement between the measured addition constants and the calculated activation barriers. The 4-methoxybenzoyl radical (**B3**) has a nearly 2 times higher addition rate constant than that of 4-morpholinobenzoyl (**B5**). This is mirrored by the considerably (50%) lower activation barrier of **B3** vs **B5**. All results of the calculations using different levels of theory are summarized in the tables presented in the Supporting Information. These results indicate that the calculated barriers are very sensitive to the choice of the theoretical procedure but less sensitive to the choice of the basis set. However, all calculations predict a significantly higher barrier of (**B1**) and (**B5**) compared to (**B2**), (**B3**), and (**B4**).

Conclusions

It was shown that TR-EPR is a suitable technique to provide rate constants of addition reactions of benzoyl radicals to alkenes. Two concentration domains of reactivity have been established for the addition of benzoyl radicals to butyl acrylate. At butyl acrylate concentrations below 1.25 M, the corresponding addition constants are between 1.4×10^6 and 2.6×10^6 mol^{-1} s^{-1}, as corroborated by TR-EPR measurements at X- and W-band. This is in the same range of values as reported in previous investigations.[14,20]

Our experiments demonstrate that the apparent reaction constant of benzoyl radicals decreases at high viscosity.

Is this specific for benzoyl radicals or is this a general behavior? This question may be answered by extending these investigations to phosphinoyl and carbon-centered radicals. This, however, is not an easy task since these more reactive radicals are expected to be consumed by the alkene at shorter times, and the transient radicals may escape detection within the time window of TR-EPR experiments.

Although the kinematic viscosity of the reaction mixture drastically increases at higher alkene concentrations, no specific line-broadening from slow tumbling motion of the benzoyl radicals is observed. Apparently, the increase of macroscopic viscosity of the reaction solution (which slows down the addition reactivity) does not translate into restricted motion of the radicals in their local microenvironment. This unhindered local mobility is corroborated by the fact that the EPR spectra of spin-label TEMPO do not reveal any anisotropy over the full viscosity range. The determination of the temperature dependence of the addition reaction may offer additional insights into these observations.

Photoinitiators producing benzoyl radicals are occurring in many industrial applications. Hence, their attenuated reactivity toward acrylates at high viscosity has to be borne in mind when estimating the efficiency of the initiating radicals in resins to be applied.

Acknowledgment. G.G. is indebted to Prof. J. H. Freed (Cornell University, Ithaca, NY) for a fruitful discussion. I.G., G.R., D.H., and G.G. thank Ciba Speciality Chemicals and the Swiss National Science Foundation for financial support. A.S. and K.M. gratefully acknowledge the Deutsche Forschungsgemeinschaft (SPP 1051) for financial support.

Supporting Information Available: Summary of calculations of reaction profiles and decay curves from time-resolved W-band EPR. This material is available free of charge via the Internet at http:// pubs.acs.org.

References and Notes

(1) Turro, N. J. *Modern Molecular Photochemistry*; University Science Books: Sausalito, CA, 1991.
(2) Khudyakov, I. V.; Legg, J. C.; Purvis, M. B.; Overton, B. J. *Ind. Eng. Chem. Res.* **1999**, *38*, 3353.
(3) Rist, G.; Borer, A.; Dietliker, K.; Desobry, V.; Fouassier, J. P.; Ruhlmann, D. *Macromolecules* **1992**, *25*, 4182.
(4) Rutsch, W.; Dietliker, K.; Leppard, D.; Kohler, M.; Misev, L.; Kolczak, U.; Rist, G. *Prog. Org. Coat.* **1996**, *27*, 227.
(5) Muller, U.; Aguirre, S. *J. Prakt. Chem. Chem. Ztg.* **1992**, *334*, 603.
(6) Leopold, D.; Fischer, H. *J. Chem. Soc., Perkin Trans. 2* **1992**, 513.
(7) Weber, M.; Khudyakov, I. V.; Turro, N. J. *J. Phys. Chem. A* **2002**, *106*, 1938.
(8) Kolczak, U.; Rist, G.; Dietliker, K.; Wirz, J. *J. Am. Chem. Soc.* **1996**, *118*, 6477.
(9) Jockusch, S.; Turro, N. J. *J. Am. Chem. Soc.* **1999**, *121*, 3921.
(10) Jockusch, S.; Turro, N. J. *J. Am. Chem. Soc.* **1998**, *120*, 11773.
(11) Gatlik, I.; Rzadek, P.; Gescheidt, G.; Rist, G.; Hellrung, B.; Wirz, J.; Dietliker, K.; Hug, G.; Kunz, M.; Wolf, J.-P. *J. Am. Chem. Soc.* **1999**, *121*, 8332.
(12) Neville, A. G.; Brown, C. E.; Rayner, D. M.; Lusztyk, J.; Ingold, K. U. *J. Am. Chem. Soc.* **1991**, *113*, 1869.
(13) Sluggett, G. W.; Turro, C.; George, M. W.; Koptyug, I. V.; Turro, N. J. *J. Am. Chem. Soc.* **1995**, *117*, 5148.
(14) Colley, C. S.; Grills, D. C.; Besley, N. A.; Jockusch, S.; Matousek, P.; Parker, A. W.; Towrie, M.; Turro, N. J.; Gill, P. M. W.; George, M. W. *J. Am. Chem. Soc.* **2002**, *124*, 14952.
(15) Brown, C. E.; Neville, A. G.; Rayner, D. M.; Ingold, K. U.; Lusztyk, J. *Aust. J. Chem.* **1995**, *48*, 363.
(16) Savitsky, A. N.; Paul, H. *Appl. Magn. Reson.* **1997**, *12*, 449.
(17) Geimer, J.; Beckert, D.; Jenichen, A. *Chem. Phys. Lett.* **1997**, *280*, 353.
(18) Bartels, D. M.; Mezyk, S. P. *J. Phys. Chem.* **1993**, *97*, 4101.
(19) Bartels, D. M.; Han, P.; Percival, P. W. **1992**, *164*, 421.
(20) Vacek, K.; Geimer, J.; Beckert, D.; Mehnert, R. *J. Chem. Soc., Perkin Trans. 2* **1999**, 2469.
(21) Savitsky, A. N.; Galander, M.; Möbius, K. *Chem. Phys. Lett.* **2001**, *340*, 458.
(22) Prisner, T. F.; Rohrer, M.; Möbius, K. *Appl. Magn. Reson.* **1994**, *167*, 7.
(23) Frisch, M. J.; Trucks, G. W.; Schlegel, H. B.; Scuseria, G. E.; Robb, M. A.; Cheeseman, J. R.; Zakrzewski, V. G.; J. A. Montgomery, J.; Stratmann, R. E.; Burant, J. C.; Dapprich, S.; Millam, J. M.; Daniels, A. D.; Kudin, K. N.; Strain, M. C.; Farkas, O.; Tomasi, J.; Barone, V.; Cossi, M.; Cammi, R.; Mennucci, B.; Pomelli, C.; Adamo, C.; Clifford, S.; Ochterski, J.; Petersson, G. A.; Ayala, P. Y.; Q. Cui; Morokuma, K.; Malick, D. K.; Rabuck, A. D.; Raghavachari, K.; Foresman, J. B.; Cioslowski, J.; Ortiz, J. V.; Stefanov, B. B.; Liu, G.; Liashenko, A.; Piskorz, P.; Komaromi, I.; Gomperts, R.; Martin, R. L.; Fox, D. J.; Keith, T.; Al-Laham, M. A.; Peng, C. Y.; Nanayakkara, A.; Gonzalez, C.; Challacombe, M.; Gill, P. M. W.; Johnson, B.; Chen, W.; Wong, M. W.; Andres, J. L.; Gonzalez, C.; Head-Gordon, M.; Replogle, E. S.; Pople, J. A. *Gaussian 98*; Gaussian, Inc.: Pittsburgh, PA, 1998.
(24) Fuhs, M.; Elger, G.; Osintsev, A.; Popov, A.; Kurreck, H.; Möbius, K. *Mol. Phys.* **2000**, *98*, 1025.
(25) Tsentalovich, Y. P.; Forbes, M. D. E. *Mol. Phys.* **2002**, *100*, 1209.
(26) Adrian, F. J.; Monchick, L. *J. Chem. Phys.* **1979**, *71*, 2600.
(27) Kaptein, R.; Oosterhoff, L. J. *Chem. Phys. Lett.* **1969**, *4*, 195.
(28) Pryor, W. A.; Smith, K. *J. Am. Chem. Soc.* **1970**, *92*, 5403.
(29) Makarov, T. N.; Bagryanskaya, E. G.; Paul, H. *Appl. Magn. Reson.* **2004**, 26, 197.

MA0483367